Available online at www.sciencedirect.com
ScienceDirect
Journal of Solid State Chemistry 181 (2008) 199–210
JOURNAL OF SOLID STATE CHEMISTRY
www.elsevier.com/locate/jssc

The synthesis of transition metal nitrides via thermolysis of metal–ammine complexes, Part I: Chromium nitride

K.S. Weil*

Materials Division, Pacific Northwest National Laboratory, Richland, WA 99352, USA

Received 14 September 2007; received in revised form 6 November 2007; accepted 12 November 2007
Available online 17 November 2007

Abstract

The thermal decomposition of a CrN precursor, hexaammine chromium(II) chloride, in ammonia has been investigated via a combination of thermogravimetric analysis, differential thermal analysis, Fourier transform infrared spectroscopy, and X-ray diffraction. Upon heating, $[Cr(NH_3)_6]Cl_2$ sequentially loses ammonia ligands, ultimately forming $CrCl_2 \cdot NH_3$ at ~400 °C. When heat-treated to 500 °C in ammonia, this compound ammonolyzes to form nanocrystalline CrN.
Published by Elsevier Inc.

Keywords: Transition metal nitride; Ammine complex; Ammonolysis

1. Introduction

The last two decades have witnessed considerable progress in the development and understanding of aqueous and non-aqueous solution-based approaches to synthesize ceramic precursors and powders. Much of this work has been driven by the potential advantages offered by these processes, including good compositional control, excellent homogeneity in the precursor, the potential to control powder morphology, low-to-moderate temperature synthesis which allows for the formation of metastable phases, and the potential to synthesize novel compounds [1–3]. Additionally, by controlling the molecular environment in solution, it is possible to regulate the reaction kinetics to yield precursors with a variety of molecular structures [4,5]. The ability to define the molecular structure and composition of the precursor, even in a limited fashion, can play an important role in how it transforms to form the final phase, potentially allowing greater control over the properties of the material [6–8]. However, it is not always possible to find a suitable precursor. This is particularly true when attempting to synthesize a compositional series of compounds, for example the substituted series $La_{1-x}Ni_xO_3$. In these cases, controlled co-precipitation is often used to prepare a multi-phasic precursor that is mixed at a nanoscale level [9]: a strategy employed in the glycine nitrate and the Pechini-type approaches of synthesizing multi-component oxide materials [10–14]. The latter technique utilizes metal–citric acid complexes that react with ethylene glycol and upon heating form metal/organic polymer precursors [14].

In synthesizing nitride compounds, particularly multi-component compositions, a number of research groups have found success using a corresponding oxide as a precursor [15–17]. Nitrides can also be readily formed via the ammonolysis of sulfide, chloride, and organometallic precursors [18,19]. More recently, the decomposition of complexed or adducted solution-formed species is being explored, because these precursors potentially offer substantial compositional control in forming multi-component nitride compounds [20–24]. Using ammine-complexed precursors, for example, we have shown that both *A*- and *B*-site cation substitution readily takes place on the layered nitride compound $CrWN_2$ [20]. In addition, complexed precursors tend to be easier to handle and less expensive than organometallics, such as metal alkyl amides [25], and they appear to convert cleanly to the target compound. The

*Fax: +1 509 375 4448.
E-mail address: scott.weil@pnl.gov

0022-4596/$ - see front matter Published by Elsevier Inc.
doi:10.1016/j.jssc.2007.11.008

complexing species are typically weakly held to the metal cations, making them thermally labile at relatively low temperatures ($T<300\,^{\circ}C$). Thus, while co-precipitation allows the metal species to be intimately mixed on a fine scale, complexation or adduct formation ensures that the metal ions are protected from hydrolysis at room temperature, but can be thermally stripped of the complexing species and reacted with a nitriding gas during subsequent heat treatment at moderate temperature [21]. In the case of ammine complexes or ammonia adducts, the precursor is a potential source of both the cation and nitrogen species.

In preparing transition metal nitrides, it is well known that transition metal halides readily react with ammonia at ~400–600 °C to form the corresponding binary nitride [26,27]. We have attempted to utilize this ammonolysis reaction to form multi-component transition metal nitrides by first stabilizing a metal halide mixture via complexation, analogous to the way chelation is employed in the original Pechini process. The target chlorides are first co-dissolved in the appropriate ratios, then co-precipitated from solution using a complexing agent such as ammonia or an organoamine [20,28–30]. This synthesis strategy has been used to prepare a variety of compounds, including MWN_2 (where $M=$Fe, Ni, Cr, Co), $(Ni_{0.8}Mo_{0.2})MoN_2$, $FeZrN_2$, $Cr_xW_{2-x}N_2$ $(1.7>x>0.6)$, $Cr(M_xW_{1-x})N_2$ (where $M=$Mo and Mn) [20]. However, the details of precursor synthesis and decomposition to form the target nitride compound have not yet been reported. Presented is the first of three papers that together describe how a multi-component nitride such as $CrWN_2$ is formed using an ammine-complexed precursor. In investigating the synthesis of this ternary compound, it was useful to first separately examine the details of chromium and tungsten nitride synthesis using ammine-complexed precursors. Here, we report on chromium nitride (CrN) formation. The synthesis of tungsten nitride and $CrWN_2$ will be discussed in two subsequent papers.

2. Experimental

2.1. Precursor synthesis and heat treatment

All chemical manipulations were conducted in an argon-filled glove box (O_2 and $H_2O\leqslant 5$ppm) or under a protective stream of ultra-high-purity nitrogen unless otherwise noted. All glassware used was acid washed with NoChromix® (Godax Laboratories) and oven dried prior to use. The reagents and solvents employed in this study were chromium(III) chloride hexahydrate ($CrCl_3\cdot 6H_2O$, 99.995%; Aldrich), anhydrous acetonitrile (CH_3CN, 99.95%; Sigma-Aldrich), and electronic-grade ammonia (NH_3, <20ppm H_2O; Mattheson Gas). As described in Ref. [20], the precursor synthesis reactions were conducted in a 500 ml three-neck round bottom reaction flask. Vacuum adapters, to which a high-temperature silicone vacuum grease (Dow Corning) was applied, were inserted into the two opposing side necks, and then sealed with parafilm. Connected to each adapter was a 10 in. length of silicone tubing that could be closed off to the ambient atmosphere by a pinch cock. The central neck of the reaction flask was sealed with a rubber septum penetrated by a metal cannula to introduce the ammonia. A Glass-Col insulated heater was used to control the temperature of the contents inside the flask. A cold trap connected to the system could be used to collect condensate and thereby separate the solvent and reaction products. The back-end of the system was connected to a series of water bubblers to monitor reaction gas flow and aid in collecting any volatile reaction by-products.

A series of precursor heat treatment experiments were conducted under flowing ammonia gas (~130 ml/min) inside of a horizontal, single-zone clamshell furnace outfitted with a 4-ft-long, 2.5-in.-diameter quartz tube. A glass end-cap at the back end of the tube furnace was connected to a mineral oil bubbler to avoid backstreaming of air and moisture into the furnace tube, while the glass end-cap at the front end of the tube was connected to pre-pure nitrogen and ammonia gas lines. For each experiment, approximately 0.5 g of the precursor powder was heated inside an aluminum nitride crucible. Prior to initiating a heat treatment run, the tube was purged for 20 min with pre-pure nitrogen, then purged an additional 10 min with ammonia. The experiments were conducted by positioning the crucible inside the quartz tube such that it sat just outside the hot zone of the furnace prior to the isothermal soak, allowing it to equilibrate with the heat treatment atmosphere at a temperature that was ~150–200 °C below the soak temperature. The quartz tube was then slid into the furnace far enough for the sample to sit in the center of the hot zone. Based on a blank run, the time required for the sample to thermally equilibrate was approximately 20–30 s. After heat treatment at the soak temperature for 0.1 h, the quartz tube was pushed back out of the furnace past its original position, so that the sample could be quickly quenched in a section of the quartz tube wrapped with a set of water-cooled coils. The following soak temperatures were used: 200, 300, 350, 400, 450, 500, 550, 600, 650, 700, and 750 °C. Once the samples were cooled, they were quickly removed from the furnace and transferred to a glove box for storage until later analysis.

2.2. Characterization

The precursor was characterized at different stages of synthesis and subsequent decomposition by several techniques to determine its original form and identify the reactions responsible for its conversion to chromium nitride. To determine the electronic and infrared spectra of the initial precursor and of the ammonolysis products as a function of reaction temperature, UV–vis and Fourier transform infrared (FTIR) spectroscopy were conducted respectively using a Perkin-Elmer Lambda 18 UV–vis spectrometer and an ATI Mattson Galaxy Series 5000 FTIR spectrometer equipped with CsI optics. The infrared

(IR) spectra were obtained in the 4000–460 cm^{-1} wave number range using the pressed KBr pellet technique. The pellets were prepared in a glove box to avoid potential contamination by air or water. The crystal structures of the heat-treated precursor powders were analyzed by X-ray diffraction (XRD) using a Rigaku θ–θ diffractometer that employed graphite-filtered Cu$K\alpha$ radiation. The XRD data for each sample were collected at a scan rate of 1.5°/min and a step size of 0.05°, typically over a 2θ range of 10–70°.

Differential thermal analysis (DTA) and thermogravimetric analysis (TGA) were conducted in a horizontal, dual cantilever Thermal Analyst DTA/TGA instrument (model TA2000). As will be discussed, the precursor was heated in three different atmospheres (air, ultra-high-purity nitrogen, and ammonia) at a rate of 3 °C/min to identify the adduct species and to determine the presence of by-product phases. Quantitative chemical analyses of the various heat-treated samples and initial precursor were performed by Galbraith Laboratories (Knoxville, TN). Inductively coupled plasma optical emission spectroscopy was used to determine the concentration of the metal species; combustion analyses were employed to evaluate the nitrogen, carbon, and oxygen contents following the American Society for Testing and Materials standard, ASTM D5373 [31], while coulometric titration was used to analyze for particularly low concentrations of these species; and ion chromatography and capillary electrophoresis techniques were used to determine the chlorine levels.

3. Results

3.1. Solid precursor synthesis and characterization

The hydrated $CrCl_3 \cdot 6H_2O$ dissolved completely within 15 min in heated (70 °C) anhydrous acetonitrile to form a transparent dark reddish-brown colored solution. During this time, a thin smoky gas slowly evolved from the solution. An aliquot of this solution was apportioned, diluted to 1/50 of its original concentration using fresh anhydrous acetonitrile, and analyzed by UV–vis spectroscopy. The resulting spectrum is shown in Fig. 1. Comparison of the values and the positions of the maxima and minima observed in this spectrum with reported literature values [32,33] for various chromous and chromic chloride solutions indicates that the hydrated chloride salt forms a nitrile-soluble acetonitrile adduct: $CrCl_2 \cdot 2CH_3CN$, which implies that the waters of hydration are lost upon dissolution and that the chromium is reduced to the +2 valence state during dissolution. The pH analysis of the water in the first bubbler at the exit of the reaction flask indicated that it was slightly acidic, suggesting that the chlorine lost upon chromium reduction was likely due to the formation of HCl gas.

Bubbling anhydrous ammonia through this solution causes immediate precipitation, although complete complexation of chromium by ammonia appears to occur somewhat more slowly, typically taking 2–3 min as evidenced by changes in the color of the precipitate during this time period, from dark red to sky blue to dark blue. XRD of the precipitate confirms the presence of NH_4Cl in the solid, as seen in Fig. 2. Apart from ammonium chloride, however, the precipitated product contains no other crystalline phases and displays only a very broad, very low intensity asymmetric hump centered at ~29°, typical of an amorphous solid. Ideally at this point, the chromium-containing precursor would be isolated from the ammonium chloride by-product in order to carry out the precursor decomposition studies. However, the intention here was to study the formation of chromium nitride as a prologue to understanding the synthesis of $CrWN_2$.

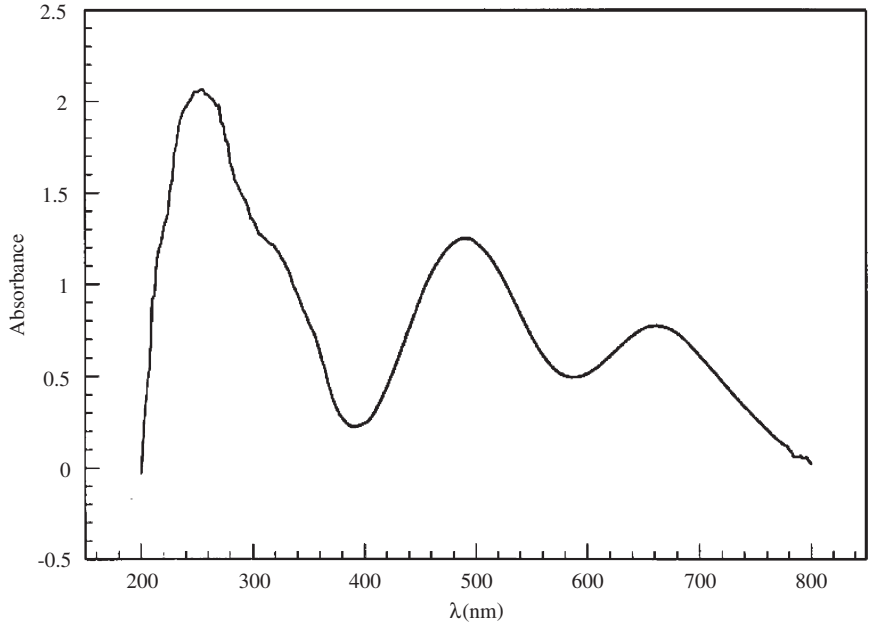

Fig. 1. The UV–vis absorption spectrum of $CrCl_3 \cdot 6H_2O$ as dissolved in anhydrous acetonitrile.

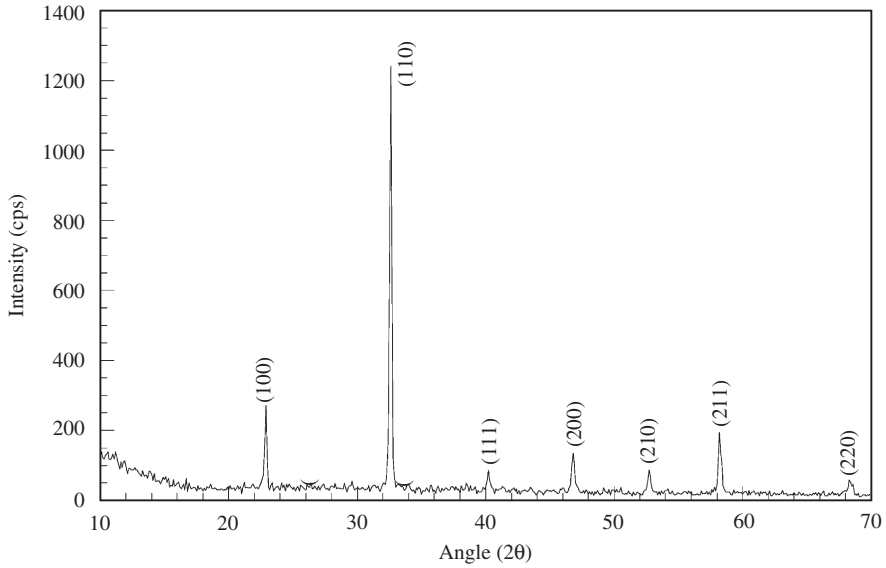

Fig. 2. The X-ray pattern collected on the ammonia-precipitated precursor. Asterisks denote the diffraction peaks for ammonium chloride (NH_4Cl).

Table 1
NH_4Cl produced during precipitation from the $CrCl_3 \cdot 6H_2O$/acetonitrile solution

Moles in acetonitrile	Moles in bubbler	Moles in precursor	Total moles	Moles of NH_4Cl per mole of Cr
0.0040	0.0018	0.0114	0.0172	0.86

Table 2
Chemical analysis of the raw precipitate

Element (wt%)					
Cr	Cl	C	N	H	O
16.53	28.87	12.16	35.01	7.24	0.19

Therefore, the amount of NH_4Cl formed due to reaction and that remaining in the raw precursor were both characterized.

In order to determine the total amount of NH_4Cl produced, three sources where the NH_4Cl could potentially collect during synthesis were analyzed: (1) the solid precursor, (2) the clear acetonitrile-based phase above the precipitated precursor, and (3) the water bubblers, attached to the outlet of the reaction vessel, initially containing de-ionized water. The precipitate and the clear supernatant liquid were separated by centrifuging the mixture at 10,000 rpm for 15 min. The precipitate was then dried under flowing argon gas at 90 °C and chemically analyzed for NH_4Cl at Galbraith Associates using a combination of titration and elemental analyses. Both the acetonitrile centrifugate and the water solution from the bubblers were heated near their respective boiling points to evaporate the solvent phases, leaving behind a white solid that was weighed and verified by XRD to be NH_4Cl. The total amount of ammonium chloride produced in this reaction was calculated by summing the amounts detected in the solid precipitate, the acetonitrile solution, and the water from the traps and equated to 0.87 mol of NH_4Cl per mole of $CrCl_3 \cdot 6H_2O$ originally introduced into the reaction vessel, as summarized in Table 1. It is assumed that some of the chlorine removed from the original chromic chloride escaped as HCl during reduction in acetonitrile. Thus, in total, approximately 1 mol of chlorine is removed from each mole of $CrCl_3 \cdot 6H_2O$ initially added to the reaction vessel. The elemental composition of the ammoniated precursor is reported in Table 2.

Fig. 3 shows the UV–vis spectrum for the raw ammoniated precursor. The three maxima and two minima observed, located, respectively, at $\lambda_{min} = \sim 200$, 409, and 564 cm^{-1}, and $\lambda_{max} = 356$ and 476 cm^{-1}, can be closely matched to the results obtained by Larkworthy and Tabatabai for $[Cr(NH_3)_6]Cl_2$ [34]. Note that NH_4Cl is essentially UV–vis insensitive [35] and has no effect on the spectrum for this precursor. To verify this conclusion, an FTIR spectrum was obtained on the solid, as shown in Fig. 4. Based on the assignments of the vibration bands detected, given in Table 3, this data provides further evidence that the chromium precipitate is a hexaammine complex. Results from chemical analysis and FTIR spectroscopy rule out a significant presence of water in the precursor (the weight percentage of oxygen in the precipitate is 0.19% as given in Table 2 and a strong H–O–H stretching mode band [36] at ~3300 cm^{-1} is not observed). Chemical analysis further suggests that approximately 2 mol of Cl per mole of Cr beyond that calculated for the amount of NH_4Cl found are present in the complexed chromium compound. It is also apparent from Table 2 that a substantial amount of carbon is present in the precursor, just over 3 mol of C per mole of Cr. The only source of carbon in this precipitation reaction

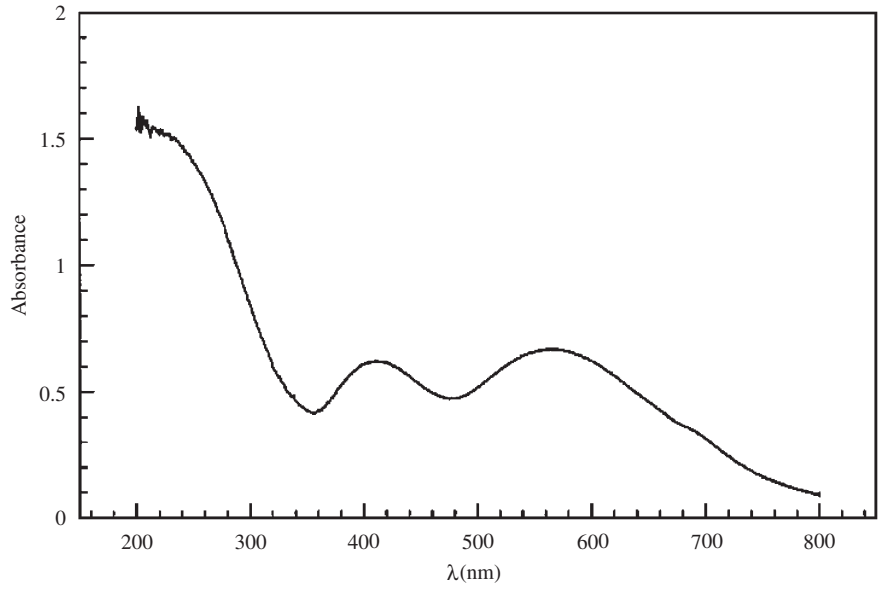

Fig. 3. The UV–vis absorbance spectrum of the ammonia-precipitated precursor.

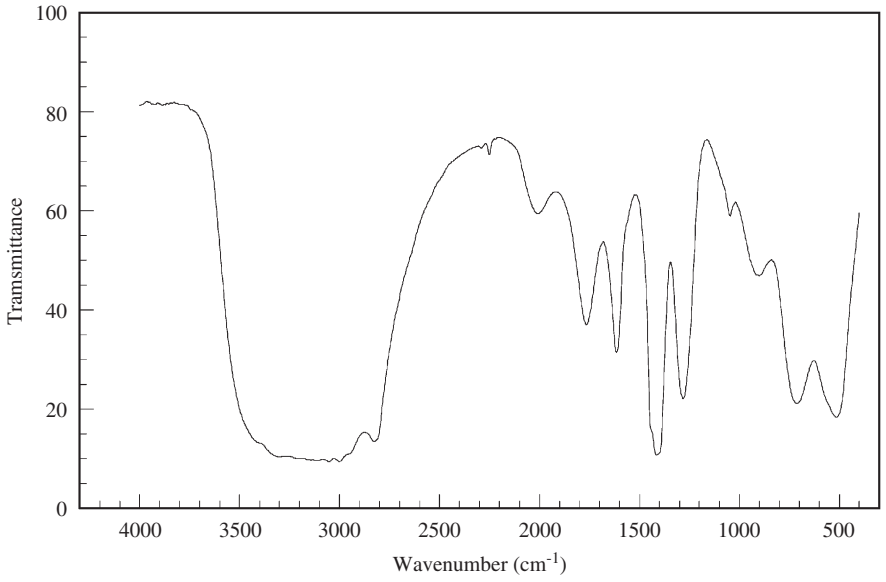

Fig. 4. The FTIR spectrum of the ammonia-precipitated precursor.

is acetonitrile. However, the presence of acetonitrile is not strongly seen in the FTIR spectrum. If CH_3CN were formally complexed to the chromium in the precursor, a strong signal arising from the $C \equiv N$ bond in acetonitrile at 2260–2240 cm^{-1} should be apparent [37]. The pattern in Fig. 4 displays a very weak vibration band at this wavelength, implying that little acetonitrile is retained in the precursor after the sample preparation process for FTIR analysis, in which the sample was allowed to thoroughly dry under a stream of ultra-high-purity Ar prior to pelletizing.

Based on these results, the crude precursor formed is composed of a mixture of $[Cr(NH_3)_6]Cl_2$ and ammonium chloride wetted by acetonitrile in a molar ratio of 1:0.57:1.59, respectively. The formation of the chromium complex is similar to that reported by Larkworthy and Tabatabai [34], who demonstrated that $[Cr(NH_3)_6]Cl_2$ is precipitated when ammonia is bubbled through ethanolic solutions of the hydrated chromium(II) halides. The molecular structure of the chromium species, $[Cr(NH_3)_6]Cl_2$, was first described by Distler and Vaughan [38] and essentially consists of a central divalent chromium ion surrounded octahedrally by the neutral ammonia species. The negatively charged chlorine ions coordinate to the resulting $Cr(NH_3)_6^{2+}$ molecule by nesting within the tetrahedral interstices formed by two opposing groups of three neighboring ammonia ligands. It should be noted that the raw precursor was not further refined prior to the

decomposition studies. Ideally one would employ a purified form of $[Cr(NH_3)_6]Cl_2$ as the starting point for investigating its ammonolysis to chromium nitride. However, there are two reasons why this was not done in this particular study. First, the larger goal of this work was to interpret the TGA, DSC, FTIR, and XRD data for the raw chromium nitride precursor as a means of understanding the formation of $CrWN_2$ and its derivatives via the ammonolysis of complexed precursors, wherein a purified mixed-metal precursor is not readily obtainable. Second, it was determined in a series of preliminary studies that NH_4Cl and acetonitrile volatilize completely during the heat treatment employed to form the target nitride compound [20].

Table 3
Assignment of the bands observed in the FTIR spectrum (Fig. 4) collected on the ammonia-precipitated precursor

Wave number (cm^{-1})	Assignment[a]	Intensity	References
3420	$\upsilon_{N-H}(NH_3)$	s	[36]
3300	$\upsilon_{N-H}(NH_3)$	s	[36]
3180	$\upsilon_{N-H}(NH_3)$	s	[36]
3050	$\upsilon_{N-H}(NH_4Cl)$	s	[37]
3000	$\upsilon_{N-H}(NH_4Cl)$	s	[37]
2830	$\upsilon_{N-H}(NH_4Cl)$	s	[37]
2240	$\upsilon_{C-N}(CH_3CN)$	vw	[37]
2010	$\delta(NH_4Cl)$	w	[37]
1770	$\delta(NH_4Cl)$	m	[37]
1610	$\delta(NH_3)$	m	[36]
1410	$\delta(NH_4Cl)$	s	[37]
1270	$\upsilon_{Cr-N}(Cr-NH_3)$	s	[36]
1040	$\delta_s(NH_3)$	w	[36]
900	$\rho_r(NH_3)$	m	[36]
710	$\rho_r(NH_3)$	s	[36]
510	$\delta(Cr-NH_3)$	s	[36]

[a] υ denotes the stretching mode, δ denotes the deformation mode, and ρ_r denotes the rocking mode.

3.2. Precursor thermolysis

TGA/DTA analyses of the precursor conducted in both flowing helium and flowing air support the calculated composition of the raw precipitate. The DTA/air thermogram in Fig. 5 displays a series of four endotherms prior to the large exotherm associated with oxidation at 360 °C: (1) two shallow asymmetric endotherms at 111 and 195 °C, (2) a sharp symmetric endotherm at 224 °C, and (3) a third shallow asymmetric endotherm at 326 °C. The accompanying weight losses measured at 111, 195, and 224 °C correspond quite closely to the loss of the volatile CH_3CN and NH_3 species (Fig. 6). Note that in the weight loss calculations, the 100% weight point was accorded to the solid at 120 °C, i.e. normalized to the stable solid obtained after drying, as shown by the horizontal line in Fig. 6. In theory, the composition of this solid should be 1 mol $[Cr(NH_3)_5]Cl_2 + 0.57$ mol NH_4Cl, since the acetonitrile should be completely evaporated at this point and $[Cr(NH_3)_6]Cl_2$ is known to lose 1 mol of NH_3 at temperatures as low as 0 °C [34].

Wendlandt and co-workers found similar DTA patterns for a number of the first row transition metal hexaammine chlorides, where a sharp endotherm at approximately 200–250 °C is generally preceded by a broad, shallow endotherm centered around 150–190 °C [39,40]. Edwards and Fowles observed a similar sequence for ammine-complexed molybdenum halide compounds [41]. Correlating the results of Wendlandt and co-workers with the thermogravimetric data shown in Fig. 6, the acetonitrile

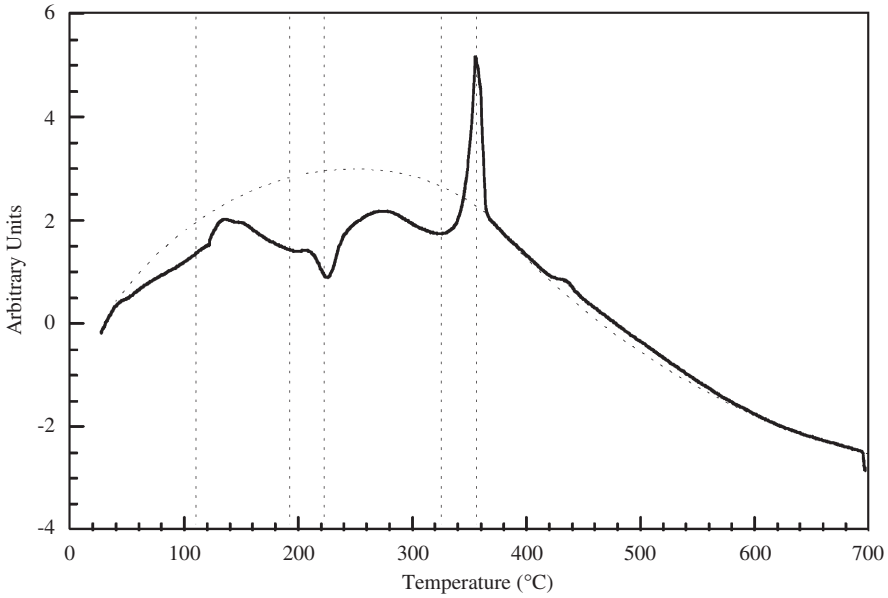

Fig. 5. Differential thermal analysis of the ammonia-precipitated precursor in flowing air (40 cm^3/min). The curved dotted line represents the calibrated background line against which the experimental thermogram is compared. The vertical lines approximately mark the thermal events in this experiment.

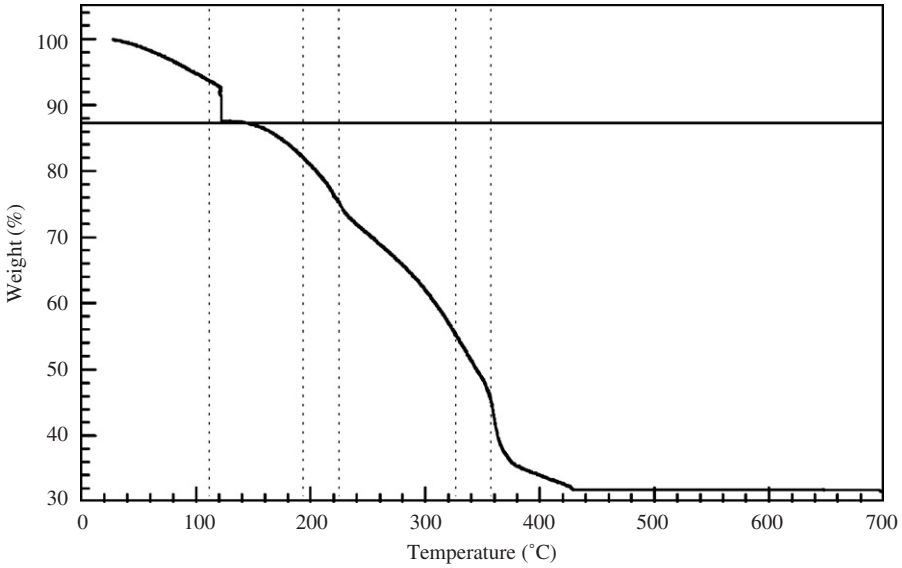

Fig. 6. Thermogravimetric analysis of the ammonia-precipitated precursor in flowing air (40 cm^3/min). The vertical lines correspond to thermal events marked in the DTA thermogram in Fig. 5.

Table 4
Cumulative weight loss in Figs. 6 and 8 as a function of heat treatment temperature

	Temperature[a]					
	⩽120 °C	195 °C	224 °C	326 °C	360 °C	600 °C
TGA in air (%)	12.2	6.9[b]	15.4	36.1	47.1	68.1
TGA in He (%)	12.3	6.8[b]	15.5	35.9	45.3	–
Expected (%)	12.8	7.2[b]	14.3	35.8	48.7	68.0
Group(s) lost	1.59 mol CH_3CN + 1 NH_3	1 NH_3[b]	1 NH_3	3 NH_3	0.57 mol NH_4Cl	Oxidation to Cr_2O_3

[a]The temperatures given here correspond to the vertical lines in Figs. 5 and 6.
[b]The weight losses are cumulative starting above 120 °C and are given as the percentage of the weight of the precursor found after the 120 °C hold, as described in the text.

and ~1 NH_3 group are lost by 120 °C. Two more NH_3 groups are lost at the next two endotherms, one group at each. Three additional NH_3 groups are thermolyzed at the 326 °C endotherm. The sublimation temperature of ammonium chloride is 340 °C [42], but its vapor pressure is significant at temperatures as low as 270 °C [42]. It appears that nearly all of the NH_4Cl in the raw precursor sublimes by 350–360 °C. The experimentally measured weight loss of the precipitate upon full oxidation (68%) compares very well with the theoretical weight change expected for the conversion of the precursor to Cr_2O_3 and volatiles. A comparison between the expected weight loss for the raw precipitate and the values found experimentally in air is provided in Table 4. The TGA/DTA experiments conducted in helium display endotherms at temperatures similar to, but generally somewhat lower than, those found in the air experiments, as shown in Fig. 7. The thermal lag observed in the air experiments when compared to those conducted in helium can be attributed to the large difference in heat transfer characteristics (i.e. thermal conductivity) between the two gases. Weight loss measurements at the lower temperatures ($T<350$ °C) compare very well with those found in the air experiments and those expected from calculation for the raw precursor, as shown in Fig. 8 and given in Table 4.

Thermogravimetric analysis of the raw precipitate in ammonia was conducted by heat treating the powder under the following schedule: heating from room temperature to 120 °C at 3 °C/min, holding at 120 °C for 1 h, and heating to 750 °C at 3 °C/min. The resulting thermogram and its derivative with respect to time are shown in Fig. 9. In general, up to 350 °C, the pattern of weight loss is similar to the thermograms collected using flowing air and helium, implying that the same thermolysis mechanisms occur under all three atmospheres. However, most of the thermolysis events are delayed by 60–90 °C in the ammonia thermogram. In this case, the observed lag may be due to two factors: (1) the difference in the thermal conductivity of ammonia relative to the other two heat treatment gases and (2) the potential for back-reaction during the thermolysis of the precursor in an ammonia-containing atmosphere. The calculated stepwise weight losses observed in

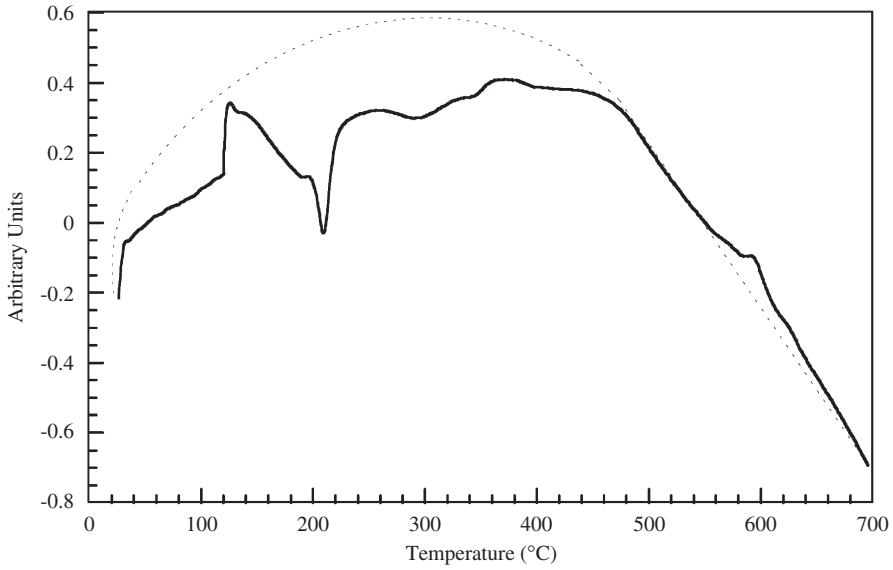

Fig. 7. Differential thermal analysis of the ammonia-precipitated precursor in flowing helium (40 cm^3/min). The curved dotted line represents the calibrated background line against which the experimental thermogram is compared.

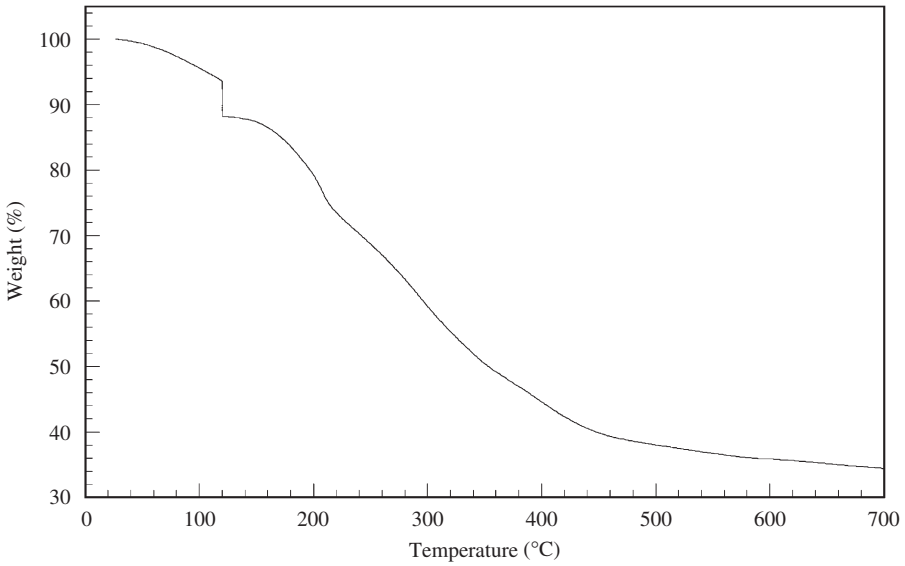

Fig. 8. Thermogravimetric analysis of the ammonia-precipitated precursor in flowing helium (40 cm^3/min).

the ammonia experiment are presented in Table 5. From the air and helium heat treatment results, it is known that $[Cr(NH_3)_6]Cl_2$ loses one NH_3 group at temperatures below 120 °C. Between 120 and 250 °C, the precursor loses one complexed ammonia group and an additional NH_3 ligand is lost by 300 °C. Between 300 and 400 °C, two more ammonia ligands are thermolyzed. The precursor then undergoes a steeper drop in weight, which begins to plateau somewhat at 475 °C, corresponding to the sublimation of the ammonium chloride impurity and the loss of the final ammonia group. The remaining chloride ammonolyzes to form chromium nitride. As will be shown, these reactions are confirmed by XRD and FTIR analyses of the residual thermolysis products.

Chemical and XRD analyses conducted on the post-TGA sample confirm that it is structured CrN crystallized in the rock-salt structure (space group: $Fm\bar{3}m$) based on the observed peaks; e.g. the curves shown in Fig. 10 for $T \geqslant 500$°C. The only other thermodynamically stable nitride previously reported for the Cr–N system, Cr_2N [43], was not observed in the ammonolyzed samples; although this does not necessarily rule out this compound as a potential intermediate in forming CrN. It has been shown that the M_2N phase commonly forms during the nitridation of many transition metal elements prior to forming MN [44]. Our result is similar to that found by Zhang et al. who investigated the ammonolysis of $CrCl_3$ and found that it forms nanocrystalline CrN at

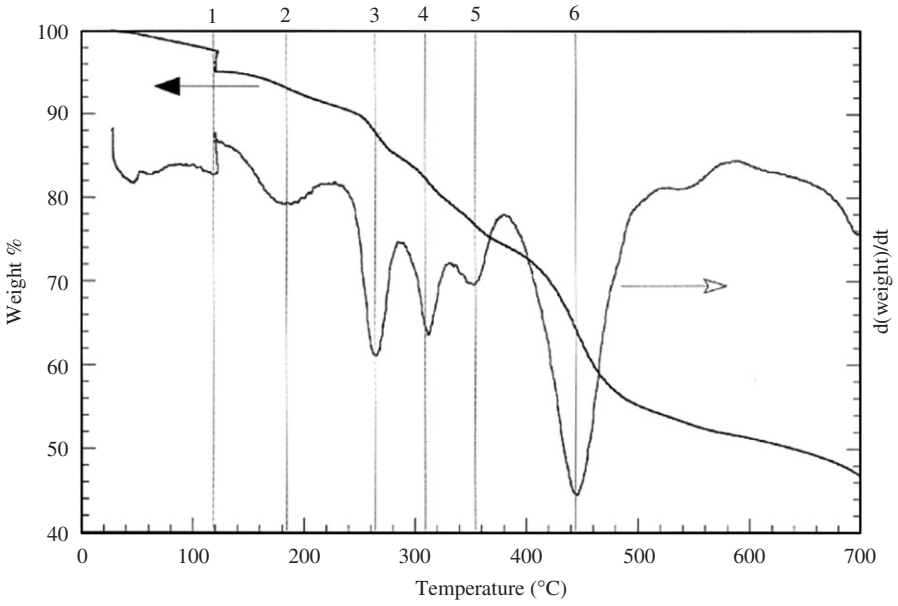

Fig. 9. Thermogravimetric analysis of the precursor in flowing ammonia (40 cm^3/min). The vertical lines approximately mark the thermal events in this experiment.

Table 5
Cumulative weight loss in Fig. 9 as a function of heat treatment temperature

	Temperature[a]					
	250 °C	300 °C	360 °C	400 °C	475 °C	700 °C
TGA in NH_3 (%)	6.8	14.7	20.7	28.4	41.1	50.5
Expected (%)	7.2	14.3	21.5	28.6	41.5	51.0
Group(s) lost	1 NH_3	1 NH_3	1 NH_3	1 NH_3	0.57 mol NH_4Cl + 1 NH_3	Nitridation to CrN

[a]The temperatures given here correspond approximately to the vertical lines in Fig. 9 and are based on the weight loss after a thermal event (i.e. after a sharp spike in d(weight)/dt). The weight losses are cumulative beginning at 120 °C and are given as the percentage of the weight of the precursor found after the 120 °C hold.

temperatures as low as 550 °C [45]. In our results, a small amount of Cl impurity (63 ppm) was detected in the final CrN compound, but no measurable amount of carbon could be determined. An average crystallite size of ~84 nm was estimated from peak width broadening calculations [46] (peak width at half-maximum intensity) using the (111), (200), and (220) peaks in Fig. 10. This result was confirmed from TEM analysis, an example of which is shown in Fig. 11. It could be argued that either $[Cr(NH_3)_5Cl]Cl$ or $CrCl_2 \cdot NH_3$ is the true precursor of CrN in this synthesis process; the first because the hexaammine loses an NH_3 group during drying and the latter because this is the final stable chlorinated compound present before CrN is found. We have chosen to refer to the hexaammine chloride as the CrN precursor, because this is the original chromium compound determined to be present in the raw precursor and in the precursor for the multi-component $CrWN_2$ compound [20].

The thermal evolution of the raw precipitate in NH_3 was also followed by conducting a series of heat treatments on the precursor, at 11 different soak temperatures for 6 min followed by quenching and characterization of the resulting powders by XRD and FTIR. The results of these analyses are shown, respectively, in Figs. 10 and 12. They confirm the thermolysis and ammonolysis mechanisms inferred from the TGA/NH_3 data. At room temperature, the only crystalline phase observed is NH_4Cl. The diffraction peaks due to this impurity are evident in the 200 and 300 °C diffractograms, although they have diminished considerably by 300 °C. By 350 °C, the NH_4Cl has almost completely sublimed. Likewise, the FTIR transmission peaks due to the ammonium chloride also disappear around this temperature, as summarized in Table 6. The FTIR peaks attributable to the coordinating NH_3 species also decrease in breadth and intensity at sequentially higher temperatures until at 450 °C, where they disappear altogether.

As is evident from the room temperature, 200 °C, and 300 °C XRD data, the complexed chromium chloride phase is initially amorphous and remains so even as it loses nearly all of the coordinating NH_3 groups. However, at 350 °C, the chloride appears to "condense", forming a poorly

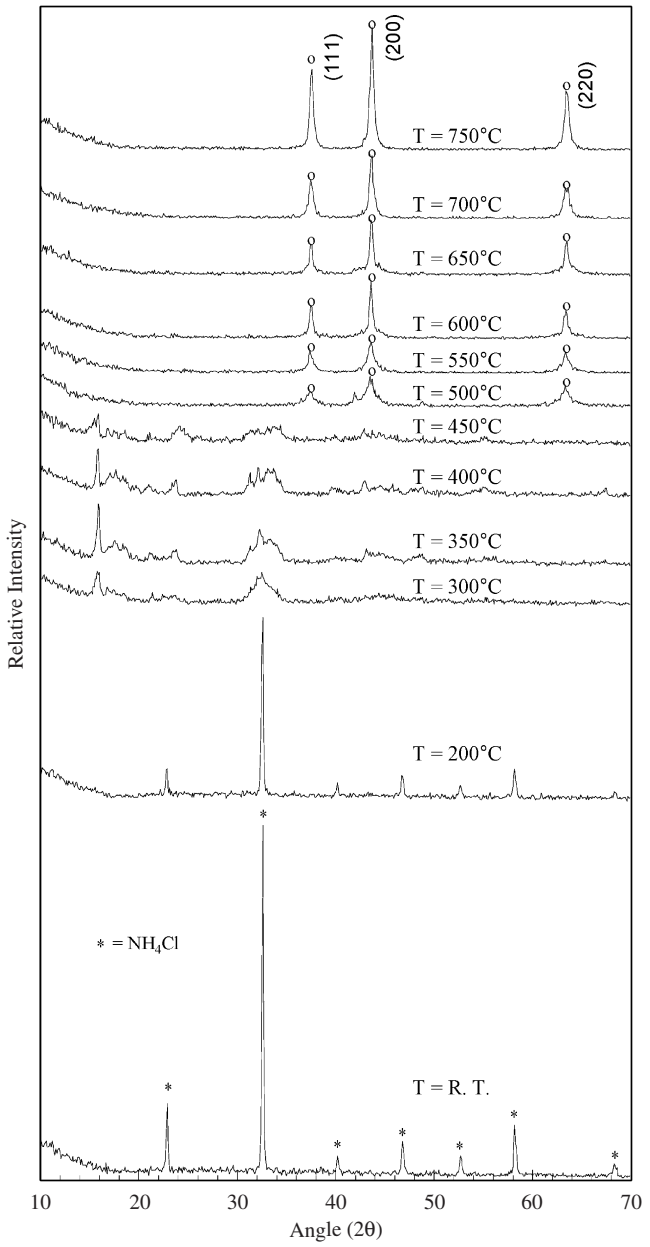

Fig. 10. XRD results displaying the evolution of the crystalline and non-crystalline phases in the precursor as a function of temperature.

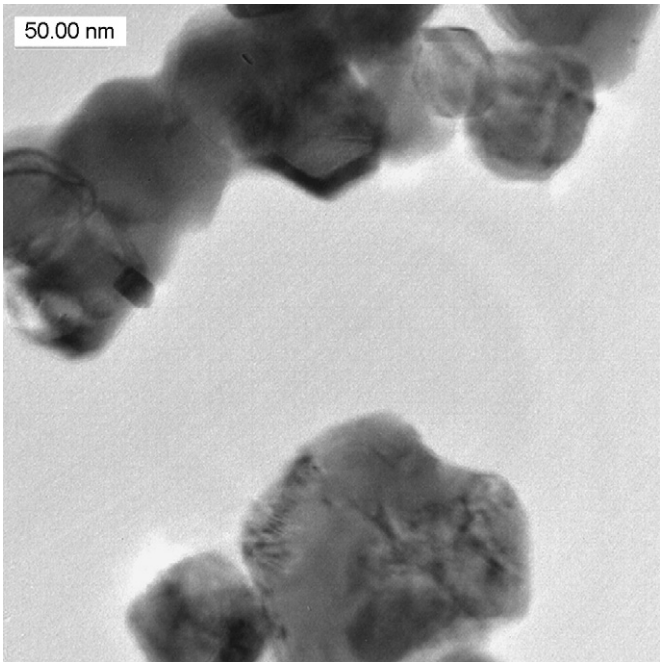

Fig. 11. TEM micrograph of the CrN product formed after ammonolysis at 500 °C for 0.1 h.

crystalline structure in which one peak at 15.2° is particularly strong. Comparison with the PDF XRD data for $CrCl_2$ suggests a possible match, although the rest of the peaks in the 350 °C diffractogram were not strong enough to confirm this [47]. More likely, the compound at this point is still partially complexed by one to two molecules of NH_3, as suggested by the TGAS/DSC data. At 500 °C, the precursor begins to undergo ammonolysis, as broad peaks (labeled in the figure) attributable to the $Fm\bar{3}m$ structured nitride, CrN, appear in the pattern. By contrast, the peaks due to the poorly crystalline phase have nearly disappeared at this temperature. These peaks of CrN narrow and grow in intensity with higher soak temperatures, suggesting a greater degree of crystallinity in this phase and growth in crystallite size with increasing heat treatment temperature.

Changes in the FTIR spectra with temperature also signal this transition. At 300 °C, the precursor begins to rapidly lose NH_4Cl, as evidenced by the disappearance of the broad vibration bands at 2830, 3000, and 3050 cm^{-1}. The presence of the N–H rocking vibrations at 1410 cm^{-1} suggests that some ammonium chloride is still left in the precursor at this temperature, though by 550 °C, this band also disappears. Note that the smaller bands at 3110, 3220, and 3310 cm^{-1} in the 300, 350, and 400 °C spectra correspond to N–H stretches of the complexing ammonia species. These were previously hidden beneath the more intense N–H peaks of ammonium chloride in the room temperature and 200 °C spectra. By 500 °C, these peaks are absent as the spectra become flat, suggesting that the heat-treated species under study have become FTIR insensitive. The likely reason for this is that the samples have become electrically conducting. Because there is no distinct band gap in an electrically conducting material, photons with energies in the infrared spectrum are absorbed simply by raising the energy of the electrons near the top of the Fermi level. That is, the photons are uniformly absorbed by the material, causing no vibration of its constituent atoms. In summary, based on the TGA, XRD, and FTIR data, it is proposed that the hexaammine chromium(II) chloride undergoes a stepwise loss of the NH_3 ligands up to ~400 °C, likely forming the monoammonia adduct species $CrCl_2 \cdot NH_3$. Around 500 °C, this species begins to ammonolyze to form nanocrystalline CrN.

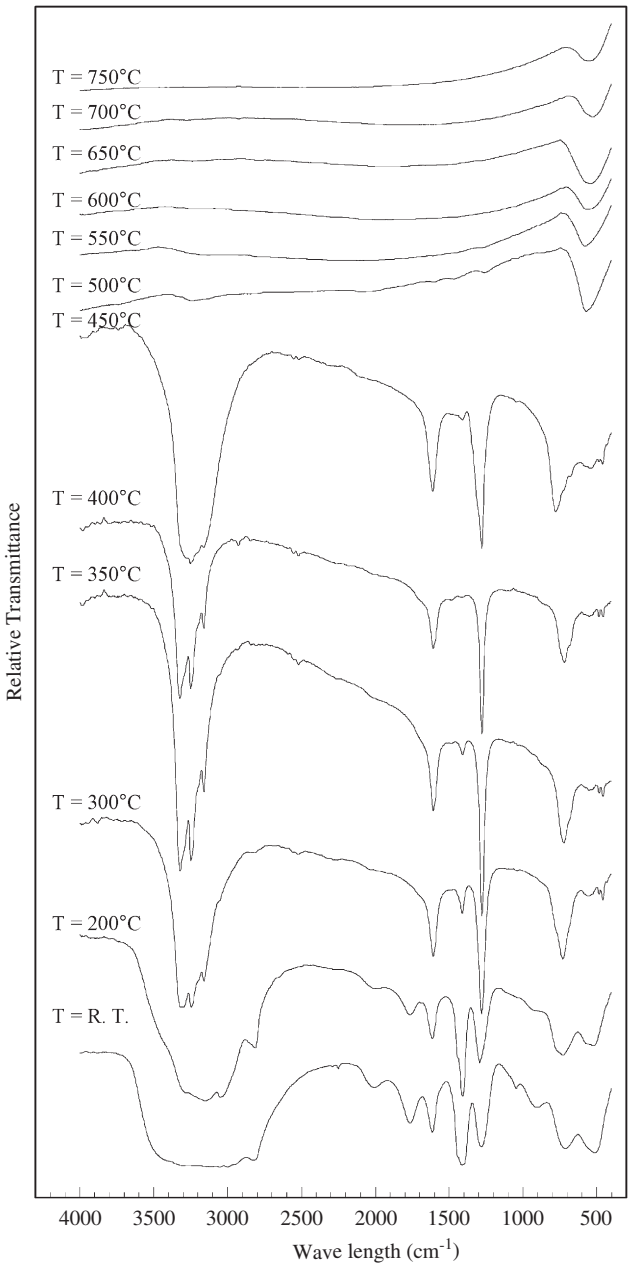

Fig. 12. FTIR results displaying the evolution of infrared spectra of the precursor as a function of temperature.

4. Conclusion

The synthesis and ammonolysis of the metal–ammine complex discussed here were examined as part of a broader study on the formation of multi-component transition metal nitrides via the complexed precursor approach. hexaammine chromium(II) chloride was precipitated via a reaction between $CrCl_2 \cdot 2CH_3CN$ and NH_3 in acetonitrile. Heating of this acetonitrile adduct species in ammonia formed stoichiometric CrN crystallized in the $Fm\bar{3}m$ structure. Upon heating, the NH_3 ligands are thermolyzed in a stepwise fashion up to ~400 °C. Slightly above this temperature ammonolysis begins to take place, forming a nanocrystalline nitride product.

Table 6
Assignment of the major bands observed in the FTIR spectra shown in Fig. 12

Wave number (cm^{-1})	Assignment	References
T = room temperature		
3050, 3000, 2830, 2010, 1770, 1410	NH_4Cl	[36]
3420, 3300, 3240, 3150, 1610, 1410	NH_3	[37]
1270, 710	NH_3	[36]
$T = 200\,^{\circ}C$		
3050, 3000, 2830, 2010, 1770, 1410	NH_4Cl	[37]
3420, 3300, 3240, 3150, 1610, 1410	NH_3	[36]
1270, 710	NH_3	[36]
$T = 300\,^{\circ}C$		
3050, 3000, 2830, 2010, 1770, 1410	NH_4Cl	[37]
3300, 3240,3150, 1610, 1410, 1270, 710	NH_3	[36]
$T = 350\,^{\circ}C$		
3300, 3240,3150, 1610, 1410, 1270, 710	NH_3	[36]
$T = 400\,^{\circ}C$		
3300, 3240,3150, 1610, 1410, 1270, 710	NH_3	[36]
$T = 450\,^{\circ}C$		
3300, 3240,3150, 1610, 1410, 1270, 710	NH_3	[36]
$T > 500\,^{\circ}C$		
Flat	Electrically conductive compound	

References

[1] J. Etourneau, Bull. Mater. Sci. 22 (1999) 165.
[2] V. Luca, J.N. Watson, M. Ruschena, R.B. Knott, Chem. Mater. 18 (2006) 1156.
[3] M.A. Beswick, N. Choi, C.N. Harmer, A.D. Hopkins, M. McPartlin, D.S. Wright, Science 281 (1998) 1500.
[4] E.R. Camargo, E. Longo, E.R. Leite, V.R. Mastelaro, J. Solid State Chem. 177 (2004) 1994.
[5] B. Tian, F. Chen, J. Zhang, M. Anpo, J. Colloid Interface Sci. 303 (2006) 142.
[6] Y.-M. Sung, K.-S. Park, S.M. Park, G.M. Anilkumar, J. Crystal Growth 286 (2006) 173.
[7] S. Mathur, H. Shen, M. Veith, R. Rapalaviciute, T. Agne, J. Am. Ceram. Soc. 89 (2006) 2027.
[8] S.-H. Yu, J. Yang, Y.-T. Qian, M. Yoshimura, Chem. Phys. Lett. 361 (2002) 362.
[9] M.-L. Fontaine, C. Laberty-Robert, A. Barnabe, F. Ansart, P. Tailhades, Ceram. Int. 30 (2004) 2087.
[10] L.A. Chick, L.R. Pederson, G.D. Maupin, J.L. Bates, L.E. Thomas, G.J. Exarhos, Mater. Lett. 10 (1990) 6.
[11] K. Deshpande, A. Mukasyan, A. Varma, Chem. Mater. 16 (2004) 4896.
[12] T. Peng, X. Liu, K. Dai, J. Xiao, H. Song, Mater. Res. Bull. 41 (2006) 1638.
[13] P.A. Lessing, Am. Ceram. Soc. Bull. 68 (1989) 1002.
[14] S. Vivekanandhan, M. Venkateswarlu, N. Satyanarayana, Mater. Chem. Phys. 91 (2005) 54.
[15] S.H. Elder, F.J. DiSalvo, L.H. Doerrer, Chem. Mater. 4 (1992) 928.
[16] J.D. Houmes, S. Deo, H.C. zur Loye, J. Solid State Chem. 131 (1997) 374.
[17] Z.X. Tang, G.C. Hadjipanayis, S.I. Shah, V. Papaefthymiou, K.J. Klabunde, J. Magn. Magn. Mater. 119 (1993) 49.
[18] F. Tessier, R. Marchand, J. Alloys Compd. 262–263 (1997) 410.

[19] C. Russel, R. Zahneisen, J. Electrochem. Soc. 139 (1992) 2424.
[20] K.S. Weil, Synthesis, structure, and properties of a novel family of layered transition metal nitride compounds, Ph.D. Thesis, Department of Materials Science and Engineering, Carnegie Mellon University, 1999.
[21] D.F. Bliss, V.L. Tassev, D. Weyburne, J.S. Bailey, J. Crystal Growth 250 (2003) 1.
[22] Y. Qiu, L. Gao, J. Am. Ceram. Soc. 87 (2004) 352.
[23] D. Choi, P.N. Kumta, J. Am. Ceram. Soc. 88 (2005) 2030.
[24] A. Gomathi, A. Sundaresan, C.N.R. Rao, J. Solid State Chem. 180 (2007) 291.
[25] G.M. Brown, L. Maya, J. Am. Ceram. Soc. 71 (1988) 78.
[26] L. Maya, Use of ammonolytic intermediates for the synthesis of nitrides and carbonitrides, DOE Report: CONF-8609120-1, 1986.
[27] S. Kaskel, K. Schlichte, T. Kratzke, J. Mol. Catal. A: Chem. 208 (2004) 29.
[28] K.S. Weil, P.N. Kumta, J. Alloys Compd. 265 (1998) 96.
[29] K.S. Weil, P.N. Kumta, J. Solid State Chem. 134 (1997) 302.
[30] K.S. Weil, P.N. Kumta, Mater. Sci. Eng. B 38 (1996) 109.
[31] ASTM D5373-02 Standard Test Methods for Instrumental Determination of Carbon, Hydrogen, and Nitrogen in Laboratory Samples of Coal and Coke, 2007.
[32] D.G. Holah, J.P. Fackler Jr., Inorg. Chem. 5 (1966) 479.
[33] A. Earnshaw, L.F. Larkworthy, K.S. Patel, J. Chem. Soc. (A) 3267 (1965).
[34] L.F. Larkworthy, J.M. Tabatabai Jr., J. Chem. Soc. Dalton Trans. 814 (1976).
[35] C.K. Jorgensen, Absorption Spectra and Chemical Bonding in Complexes, Pergamon Press, London, 1962.
[36] K. Nakamoto, Infrared Spectra of Inorganic and Coordination Compounds, second ed., Wiley, New York, 1970.
[37] R.T. Conley, Infrared Spectroscopy, Allyn & Bacon, Boston, 1966.
[38] T. Distler, P.A. Vaughan, Inorg. Chem. 6 (1967) 126.
[39] W.W. Wendlandt, J.P. Smith, J. Inorg. Nucl. Chem. 25 (1963) 985.
[40] W.W. Wendlandt, L.Y. Chou, J. Inorg. Nucl. Chem. 26 (1964) 943.
[41] D.A. Edwards, G.W.A. Fowles, J. Less-Common Met. 4 (1962) 512.
[42] CRS Handbook of Chemistry and Physics, A Ready-Reference Book of Chemical and Physical, 77th ed., CRC, Boca Raton, FL, 1996–1997.
[43] T.B. Massalski (Ed.), Binary Alloy Phase Diagrams, second ed., ASM International, 1990, p. 1293.
[44] L.E. Toth, Transition Metal Carbides and Nitrides, Academic Press, New York, 1971.
[45] Z. Zhang, R. Liu, Y. Qian, Mater. Res. Bull. 37 (2002) 1005.
[46] T. Ekström, C. Chatfield, W. Wruss, M. Maly-Schreiber, J. Mater. Sci. 20 (1985) 1266.
[47] J.W. Tracy, N.W. Gregory, E.C. Lingafelter, J.D. Dunitz, H.-C. Mez, R.E. Rundle, C. Scheringer, H.L. Yakel, M.K. Wilkinson, Acta Crystallogr. 14 (1961) 927.